Inorganic Chemistry

ARTICLE

pubs.acs.org/IC

W-Knotted Chain $\{[Cu^{II}(dien)]_4[W^V(CN)_8]\}^{5+}_{\infty}$: Synthesis, Crystal Structure, Magnetism, and Theory

Robert Podgajny,*[,†] Robert Pełka,*[,‡] Cédric Desplanches,[§] Laurent Ducasse,[∥] Wojciech Nitek,[†] Tomasz Korzeniak,[†] Olaf Stefańczyk,[†] Michał Rams,[⊥] Barbara Sieklucka,*[,†] and Michel Verdaguer[#]

[†]Faculty of Chemistry, Jagiellonian University, Ingardena 3, 30-060 Kraków , Poland

[‡]H. Niewodniczański Institute of Nuclear Physics PAN, Radzikowskiego 152, 31-342 Kraków, Poland

[§]CNRS, Université de Bordeaux, ICMCB, 87 avenue du Dr. A. Schweitzer, Pessac, F-33608, France

[∥]ISM, UMR 5255 CNRS, Université de Bordeaux, 33405 Talence cedex, France

[⊥]M. Smoluchowski Institute of Physics, Jagiellonian University, Reymonta 4, 30-059 Kraków, Poland

[#]Institut Parisien de Chimie Moléculaire, UMR 7021, CNRS, Université Pierre et Marie Curie, 75252 Paris Cedex 05, France

Supporting Information

ABSTRACT:

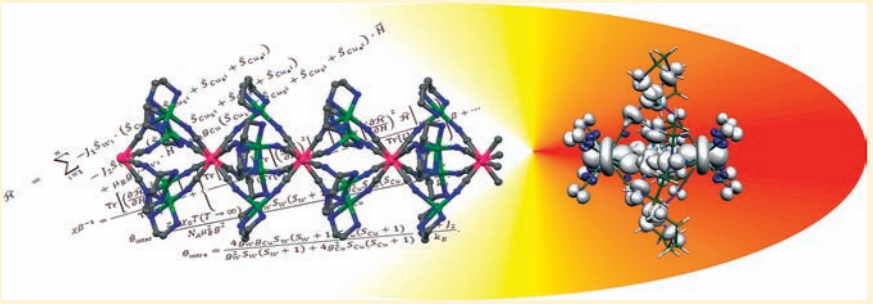

The self-assembly of $[Cu^{II}(dien)(H_2O)_2]^{2+}$ and $[W^V(CN)_8]^{3-}$ in aqueous solution leads to the formation $(H_3O)\{[Cu^{II}(dien)]_4[W^V(CN)_8]\}[W^V(CN)_8]_2\cdot 6.5H_2O$ (**1**). The crystal structure of **1** consists of an unprecedented $\{[Cu^{II}(dien)]_4[W^V(CN)_8]\}^{5+}_{\infty}$ chain of (2,8) topology, nonbridging $[W(CN)_8]^{3-}$ anions, and crystallization water molecules. The analysis of magnetic behavior of **1** was performed by the density functional theory (DFT) method and magnetic susceptibility measurements. The DFT broken symmetry approach gave two J_{CuW} coupling constants: $J_{ax} = +2.9\ cm^{-1}$ assigned to long and strongly bent W−CN−Cu linkage, and the $J_{eq} = +1.5\ cm^{-1}$ assigned to short and less bent W−CN−Cu linkage, located at the axial and the equatorial positions of square pyramidal Cu^{II} centers, respectively, in the hexanuclear $\{W_2Cu_4\}$ chain subunit. The dominance of weak-to-moderate ferromagnetic coupling within the chain was confirmed by magnetic calculations. Zero-field susceptibility of the full chain segment $\{WCu_4\}_n$ was calculated by a semiclassical analytical approach assuming that only one W^V out of five $^1/_2$ spins of the chain unit WCu_4 is treated as a classical commuting variable. The calculation of the field dependence of the magnetization was performed separately by replacing the same spin with the Ising variable and applying the standard transfer matrix technique. The intermolecular coupling between the chain segments and off-chain $[W(CN)_8]^{3-}$ entities was resolved using the mean-field approximation set to be of antiferromagnetic character. The magnetic coupling parameters are compared with those of other low dimensional $\{Cu^{II}$-$[M^V(CN)_8]\}$ systems.

INTRODUCTION

The studies of structure−property relationship in the series of magnetic compounds has been recognized as the key strategy to understanding of the principles that govern magnetic coupling in wide variety of compounds including inorganic metallic or metal-oxides materials, organic radical based materials, and coordination compounds. The last domain combining effectively the inorganic and organic building blocks was exhaustively exploited during past decades resulting in the appearance of single molecule magnets (SMM), single chain magnets (SCM), room temperature magnets, photomagnets, chiral magnets, or magnetic sponges. Among these species the octacyanide-bridged assemblies received considerable attention because of the specific binding and coupling properties of CN^- bridges implying the broad range of tunable geometrical bridging configurations, extent of magnetic interactions, and structural/magnetic dimensionality.[1]

Received: July 5, 2010
Published: March 16, 2011

Within this line, copper(II)-octacyanidometalate(V,IV) Cu^{II}-$[M^{V,IV}(CN)_8]^{3-/4-}$ (M = Mo, W) complexes have attracted interest because of the occurrence of long-range magnetic ordering below T_c temperatures tunable by various external stimuli,[2−4] making them useful for developing new multifunctional materials.[5] The magnetic exchange interaction within the $M^{V}_{(S=1/2)}-CN-Cu^{II}_{(S=1/2)}$ linkage leads to layered magnets with T_c up to 40 K with metamagnetic behavior.[1] The bilayered magnets with coordination skeleton of general formula $\{Cu^{II}[W^{V}(CN)_8]\}^{-}_{\infty}$ were studied in detail.[2c−e,3] Magnetic anisotropy originating from the presence of easy plane of magnetization parallel to the bilayer and hard axis of magnetization perpendicular to the bilayer were evidenced in the single crystals of $(tetrenH_5)\{[Cu^{II}_5[W^{V}(CN)_8]_5\}\cdot 9H_2O$ (tetren = tetraethylenepentamine).[3d] The energy of the antiferromagnetic → ferromagnetic spin flip of 4.8×10^2 J·m^{-3} was theoretically estimated[2e] to be in agreement with the value of the critical magnetic field of spin flip of ∼80−200 Oe observed experimentally for these family of compounds. The photomagnetic studies have been centered on light irradiation of cyanido-bridged paramagnetic $\{Cu^{II}[Mo^{IV}(CN)_8]\}$ species, which resulted in the appearance of magnetically ordered phases for 3-dimensional networks[4] and high spin molecules for 0-dimensional systems.[6] This effect was interpreted in terms of the formation of reversible metastable excited states: $Cu^{II}_{(S=1/2)}Mo^{V}_{(S=1/2)}Cu^{I}_{(S=0)}$[6a−e] in case of visible laser light as well as $Cu^{II}_{(S=1/2)}{}^{*}Mo^{IV}_{(S=1)}Cu^{II}_{(S=1/2)}$[6f] in the case of X-ray synchrotron radiation. Other studies focused on the reversible structural changes induced by water/*n*-propanol exchange that lead to the modulation of magnetic exchange pathways and thus, of the overall magnetic state of the Cu^{II}-pym-$[W(CN)_8]^{3-}$ (pym = pyrimidine) three-dimensional (3D) framework.[2g] The function of chirality was implemented for magnetic networks using chiral ligands to show the significant differences in the nature of long magnetic interaction between chiral $[W(CN)_8]_4[Cu\{(S \text{ or } R)\text{-pn}\}H_2O]_4[Cu\{(S \text{ or } R)\text{-pn}\}]_2\cdot 2.5H_2O$ and racemic $[W(CN)_8]_4[Cu\{(rac)\text{-pn}\}H_2O]_4[Cu\{(rac)\text{-pn}\}]_2\cdot 2.5H_2O$ layered magnets (pn = 1,2 diaminopropane).[2b,h] Very recently, the use of anisotropic $\{Cu^{II}Ln^{III}L\}^{n+}$ (Ln = lanthanide, L = tetradentate ligands) dinuclear building blocks allowed for the construction of trimetallic $\{Cu^{II}Ln^{III}L\}[M^{V}(CN)_8]$ and $\{Cu^{II}Ln^{III}L\}[M^{V}(CN)_8]$ low dimensional systems revealing slow magnetic relaxation characteristics.[7]

In this context, an important objective in this field is the reliable theoretical estimation of the parameters of a short-range interaction within the $M^{V}_{(S=1/2)}-CN-Cu^{II}_{(S=1/2)}$ linkage.[2g,3d,7a,8] This can be achieved by the estimation of the exchange coupling constants J in low dimensional $M^{V}-CN-Cu^{II}$ assemblies whose finite size and low nuclearity allow the application of the theoretical model for calculation of the intermetallic M(V)-Cu(II) coupling. In a our recent contributions we studied the magnetic exchange interactions in the discrete species $\{CuW\}^{-}$, $\{Cu_2W\}^{+}$, and $\{Cu_2W_2\}^{2-}$.[8b−d] For $W^{V}-CN-Cu^{II}$ linkages we noted the dominance of ferromagnetic W−Cu coupling for equatorial cyanido bridges at Cu(II) centers, with coupling constants ranging from +30 to +40 cm^{-1}. For the axial cyanido bridges, the apparent antiferromagnetic contribution increases, which leads to lowering of J below +10 cm^{-1} [7a,8c] or even to small negative values.[8a,b] The correlation of the J_{CuW} parameters calculated for $[Cu^{II}(phen)_3]_2[Cu^{II}(phen)_2(\mu\text{-NC})_2W^{V}(CN)_6]_2(ClO_4)_2\cdot 10H_2O$ and $[(Cu^{II}(bpy)_2(\mu\text{-NC}))_2W^{V}(CN)_6][Cu^{II}(bpy)_2(\mu\text{-NC})W^{V}(CN)_7]\cdot 5H_2O$ with the geometry of cyanido bridges at copper(II) centers based on the density functional theory (DFT) calculations confirmed the experimental results.[8d] The DFT calculations revealed also the small overlap between the magnetic orbitals of copper(II) and tungsten(V) in these compounds.

To extend the magneto-structural correlation to low dimensional Cu^{II}-$[W^{V}(CN)_8]^{3-}$ architectures, we carried out the reaction of $[W^{V}(CN)_8]^{3-}$ with Cu^{II} ions in the presence of dien (dien = diethylenetriamine). By introducing the $[Cu^{II}(dien)(H_2O)_2]^{2+}$ fragment, which has a strong preference to form $[Cu(dien)(NC)_2]^{2+}$ moieties of square pyramidal geometry with the cyanido bridges at equatorial and axial sites,[9] we have obtained $(H_3O)\{[Cu^{II}(dien)]_4[W^{V}(CN)_8]\}[W^{V}(CN)_8]_2\cdot 6.5H_2O$ (**1**). The reported compound is the first one consisting of the unique cyanido-bridged W-knotted chain $\{[Cu^{II}(dien)]_4[W^{V}(CN)_8]\}^{5+}_{\infty}$. The broken symmetry DFT calculations for the selected $\{W_2Cu_4\}$ unit and numerical analysis of magnetic data indicate weak ferromagnetic interactions through CN^{-} ligands within the chain. The possible factors influencing J_{CuW} values are discussed.

EXPERIMENTAL SECTION

Materials and Synthesis. $CuCl_2\cdot 2H_2O$, diethylenetriamine, and other chemicals were obtained from the commercial sources (Sigma-Aldrich, Idalia) and used without further purification. $Cs_3[W(CN)_8]\cdot 2H_2O$[10] were synthesized according to the literature procedures. An aqueous solution of $[Cu^{II}(dien)(H_2O)_2]Cl_2$ was obtained by mixing equimolar aqueous solution of $CuCl_2\cdot 2H_2O$ (0.6 mmol, 0.103 g, 2 mL) and diethylenetriamine (0.6 mmol, 63 μL).

$(H_3O)\{[Cu^{II}(dien)]_4[W^{V}(CN)_8]\}[W^{V}(CN)_8]_2\cdot 6.5H_2O$ 1. The best crystals of **1** were obtained by a slow diffusion of aqueous solutions (pH = 5.5) of $[Cu^{II}(dien)(H_2O)_2]Cl_2$ (0.6 mmol, 2 mL) and the $Cs_3[W^{V}(CN)_8]\cdot 2H_2O$ (0.4 mmol, 0.333 g, 2 mL) in an H-tube at room temperature. The crystals were filtered off and washed with water and ethanol and air-dried. The crystals of **1** obtained in this manner were contaminated with very small blue crystals, which were not identified. The purification in the ultrasonic bath (10 s) allowed to get rid of the superficial contamination, which was verified under the optical microscope (40 times magnification). Yield: 60 mg, 22%. Elementary analysis (Found: C, 24.4; N, 25.2; H, 3.8. Calcd for $C_{40}H_{68}N_{36}O_{7.5}Cu_4W_3$: C, 24.3; N, 25.5; H, 3.5%). The thermogravimetric analysis (TGA/DTG) coupled with a quadrupole mass spectrometer (QMS): weight loss up to 125 °C found: 6.54%, m/z = 18, H_2O^{+}; weight loss calculated for $C_{40}H_{68}N_{36}O_{7.5}Cu_4W_3$, (7.5 H_2O): 6.82%. IR: ν(O−H), 3431vs(br); ν(N−H), 3327s, 3278s; ν(C−H), 2965w, 2928w, 2887w; ν(C≡N), 2180w(sh), 2166 m, 2150 m, 2128s; δ(O−H), δ(N−H) 1620w(sh), 1590s, 1493vw; δ(C−H), ν(C−C), ν(C−N), 1456 m, 1395 w, 1318w, 1292w, 1256w, 1134w, 1085s, 1046vw, 1023vs, 987w; γ(C−H), γ(N−H), γ(O−H), 916w, 897w, 833vw, 658 m; ν(Cu−N), ν(W−C), 516 m, 480 m, 457w. The ν(CN) stretching frequencies of 2180w, 2166 m, 2150 m and 2128s cm^{-1} in IR spectra are in agreement with the presence of bridging $W^{V}-CN-Cu^{II}$ and nonbridging $W^{V}-CN$ coordination modes of CN^{-}.[11] No Cs^{+} ions were detected by X-ray microanalysis.

X-ray Crystallography. The single crystal diffraction data were collected on a Nonius Kappa CCD equipped with a Mo Kα radiation source and graphite monochromator. The space group was determined using the ABSEN[12] program. The structure of **1** was solved by direct methods using SIR-97.[13] Refinement and further calculations were carried out using SHELXL-97.[14] The non-H atoms, with exceptions of water molecules (O2−O7) and disordered C and N atoms of nonbridging $[W(CN)_8]^{3-}$ (CN34, CN37, and CN38) were refined anisotropically using weighted full-matrix least-squares on F^2. All hydrogen atoms bonded to carbon atoms of organic components were positioned with an idealized geometry and refined using a riding model with U_{iso}(H) fixed

Table 1. Selected Crystallographic Data for 1

	1
empirical formula	$C_{40}H_{32}Cu_4N_{36}O_{10.5}W_3$
formula weight	1990.73
crystal system	tetragonal
space group	$P4/n$
unit cell dimensions/Å	a = 24.2059(3)
	b = 24.2059(3)
	c = 13.3200(2)
volume/Å^3	7804.50(18)
Z	4
density, calc./Mg·m^{-3}	1.694
temperature/K)	293(2)
absorption coefficient/mm^{-1}	5.538
wavelength/Å	0.71073
F(000)	3784
crystal size/mm^3)	0.40 × 0.10 × 0.10
θ range for data collection (deg)	1.68 to 26.75
index ranges	$-30 \le h \le 30$
	$-28 \le k \le 30$
	$-16 \le l \le 9$
reflection collected	43461
independent reflections	8294 [R(int) = 0.0600]
completeness to θ = 26.75°	99.7%
absorption correction	semiempirical from equivalents
max. and min transmission	0.6074 and 0.2154
refinement method	full-matrix least-squares on F^2
data/restraints/parameters	8294/30/393
goodness of the fit on F^2	1.015
final R indices [$I > 2\sigma(I)$]	R_1 = 0.0719, wR_2 = 0.1902
R indices (all data)	R_1 = 0.0977, wR_2 = 0.2152
largest diff. peak and hole e·Å^{-3}	7.539 and −3.548

at 1.2U_{eq}(C). Hydrogen atoms of crystallization water molecules were not located. Structural diagrams were prepared using Mercury 1.4.2 software. Selected crystallographic data for **1** are shown in Table 1. The nonbridging $[W(CN)_8]^{3-}$ and crystallization water molecules reveal some degree of distortion. The structural model for **1** requires the total charge balance +1 for one $Cu_4W_3^{-1}$ unit. This requirement may be fulfilled by the assumption of the existence of the interstitial H_3O^+ cations, because of the experimental conditions employed (acidic conditions).

Physical Techniques. Elemental analyses (C, H, N) were performed on a EuroEA EuroVector Elemental Analyzer. Thermogravimetric data in the temperature range 25−400 °C were collected on a Mettler Toledo TGA/SDTA 851e microthermogravimeter equipped with QMS Thermostar GSD 300 T Balzers at heating rate of 5 °C min^{-1} in Ar atmosphere. IR spectra were measured in KBr pellets between 4000 and 400 cm^{-1} using a Bruker EQUINOX 55 FTIR spectrometer. Magnetic susceptibility χ_{dc} measurement versus temperature T, at magnetic field H = 1000 Oe and versus magnetic field H at T = 2 K, was performed using a Quantum Design SQUID magnetometer.

Computational Methods. The *Continuous Shape Measure* analysis was performed using the SHAPE v. 2.0 software.[15] Calculations of magnetic susceptibility and isothermal magnetization of **1** are performed assuming the molecular-field approximation to account for the intermolecular interaction between the chain segments and the off-chain $[W(CN)_8]^{3-}$ entities. The chain part of the spin system is solved using the model developed by Curély and Georges[16] for an isotropic chain, where a single moment $\vec{S}_i$ which is treated classically, alternates with a composite subsystem of quantum and/or classical spins Ψ_i. The Hamiltonian for each subsystem Ψ_i is rigorously diagonalized. Because of the isotropy of exchange interactions within the chain upon the expansion in Legendre polynomials a closed-form expression for the zero-field susceptibility is obtained. The chain part of the magnetization is calculated using the transfer matrix technique upon replacement of the spin of each W^V ion by the Ising-like variable. The calculations were encoded in two notebooks prepared in the *Mathematica8.0* environment. The fitting procedures incorporated the in-built *Mathematica* function *FindMinimum*. Standard DFT calculations have previously been used for the evaluation of exchange coupling constants for transition metal dinuclear complex, including some of the second-row transition series.[17] The DFT energies were calculated using the unrestricted hybrid B3LYP functional[18] together with the D95 Dunning−Huzinaga valence double-ζ basis set[19] for C, H, and N and for the first-row transition elements and the LANL2DZ small-core Hay−Wadt pseudopotential[20] for transition metals. The procedure developed by Ruiz et al.[21] has been used. All the calculations were performed using the Gaussian03 code.[22] The magnetic orbitals employed here have been drawn from the ferromagnetic ground state. In restricted calculations, the same orbital is used for spin up and spin down electron, so that the orbital to be drawn are simply the so-called singly occupied molecular orbitals (SOMOs). However such calculations do not allow to estimate J coupling constants, being especially unable to reproduce spin-polarization. In unrestricted calculations, the molecular orbitals for α and β electrons are allowed to be different. Orbital to be checked *a priori* should be occupied α orbitals of high energy (occupied magnetic spin−orbitals, OMSOs). However, it has been previously shown[23] that these orbitals were usually exceedingly delocalized toward the ligands. Hence, to avoid the use of such overdelocalized orbitals, the unoccupied magnetic spin−orbitals (UMSOs), the low energy β molecular orbitals, have been represented.[23]

RESULTS AND DISCUSSION

Crystal Structure. The crystal structure of $(H_3O)\{[Cu^{II}(dien)]_4[W^V(CN)_8]\}[W^V(CN)_8]_2\cdot 6.5H_2O$ (**1**) is built from the cyanido-bridged chains $\{[Cu^{II}(dien)]_4[W^V(CN)_8]\}^{5+}_{\infty}$ running parallel to the c crystallographic axis, nonbridging $[W(CN)_8]^{3-}$ anions, interstitial H_3O^+ cations, and crystallization H_2O molecules (Figure 1). The most important distances and angles are presented in Table 2. Detailed metric parameters are given in the Supporting Information, Table S1. The chain is formed by $[W(CN)_8]^{3-}$ located on the C_4 axis, which coordinates eight adjacent Cu(II) centers through cyanido ligands, C-bonded to tungsten (Figure 1b) with W−C and C−N distances and W−C−N angles typical for this complexes.[2−4,6−8] Two crystallographically different bridging $[W(CN)_8]^{3-}$ anions, W(1) and W(2), alternate in the chain with W(1)···W(2) intramolecular distances of 6.62 Å. The exact description of the relevant polyhedra is provided by *continuous shape analysis* parameters[24] and indicates that $[W(1)(CN)_8]^{3-}$ and $[W(2)(CN)_8]^{3-}$ polyhedra are similar to each other and have a geometry very close to the ideal square antiprism (D_{4d}, SAPR-8). The sets of four Cu(4) and four Cu(5) copper centers aligned alternatively between the W(1) and W(2) tungsten sites are arranged in squares perpendicular to the axis of the chain and parallel to the square planes of N atoms in the $[W(CN)_8]^{3-}$ moieties. The interatomic distances Cu(4)···Cu(4) and Cu(5)···Cu(5) within one square are 5.78 and 5.73 Å, respectively, while the Cu(4)···Cu(5) distances between two neighboring squares are in the range 7.30−7.40 Å (Supporting Information, Figure S1). Distances and angles of $[Cu(dien)(NC)_2]$

dx.doi.org/10.1021/ic101335a |*Inorg. Chem.* 2011, 50, 3213–3222

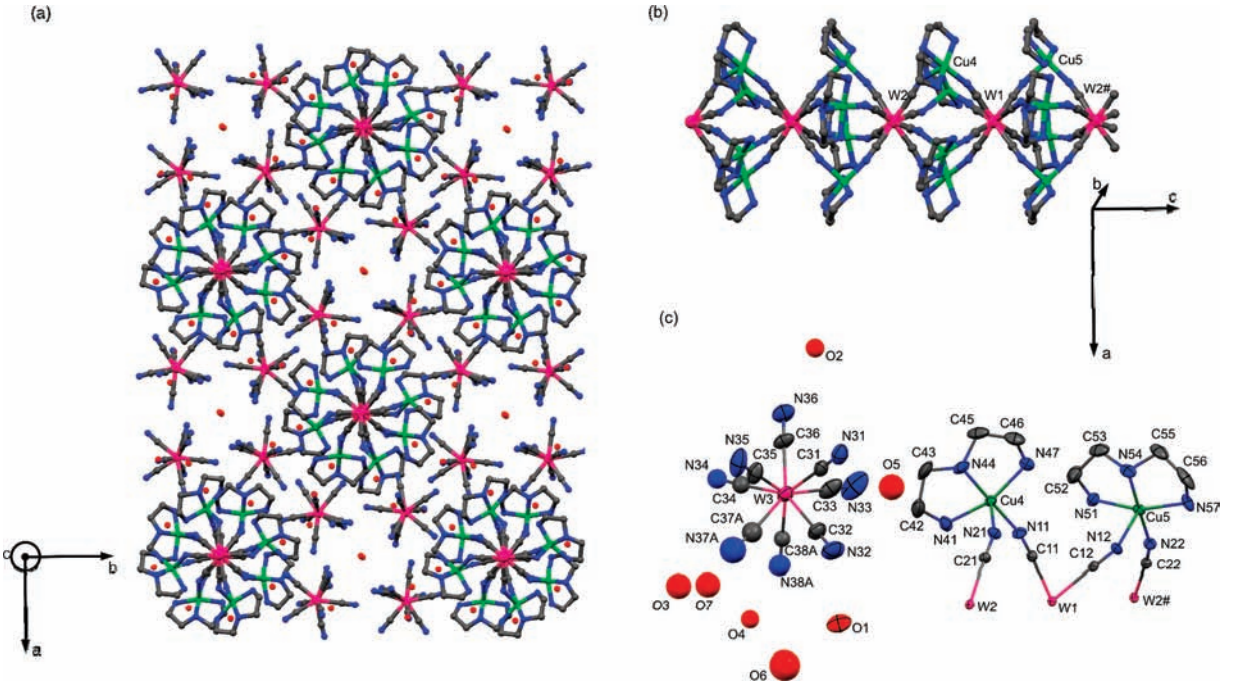

Figure 1. Crystal structure of **1**: (a) the packing diagram, a view down the *c* crystallographic direction; (b) chain structure of $\{[Cu^{II}(dien)]_4[W^V(CN)_8]\}^{5+}{}_\infty$; (c) atom labeling scheme with 30% ellipsoid probabilities. Colors: W, pink; Cu, green; C, gray; N, blue; O, red. Hydrogen atoms are omitted for clarity.

Table 2. Most Important Bond Lengths [Å] and Angles [deg] in Cyanido-Bridged Linkages in 1

W(1) and W(2) Moieties			
W−C range/average		2.152−2.167/2.158	
N−C range/average		1.128−1.156/1.143	
W−C−N range/average		173.7−178.3/176.1	
Cu(4) Moiety			
Cu(4)−N(11)	1.960(8)	C(11)−N(11)−Cu(4)	166.8(9)
Cu(4)−N(21)	2.290(8)	C(21)−N(21)−Cu(4)	143.3(8)
Cu(5) Moiety			
Cu(5)−N(12)	2.233(8)	C(12)−N(12)−Cu(5)	145.9(8)
Cu(5)−N(22)	1.969(8)	C(22)−N(22)−Cu(5)	160.3(8)

moieties of square pyramidal geometry are practically identical to those found in $[Cu(dien)]_3[Fe(CN)_6]_2\cdot 6H_2O$ and similar structures.[9] In $[Cu(dien)(NC)_2]$, Cu(II) coordinates at short distances the three nitrogens of the dien ligand and one nitrogen of a cyanido bridge at the equatorial site [Cu(4)−N(11), 1.960(8) and Cu(5)−N(22), 1.969(8) Å], and at significantly longer distances cyanide bridge at the axial site [Cu(4)−N(21), 2.290(8) and Cu(5)−N(12), 2.233(8) Å]. These two sets of distances are related to two different non linear geometries of W−CN−Cu linkages. The (W-)C−N−Cu unit is less bent in short equatorial CN bridges [C(11)−N(11)−Cu(4), 166.8(9)° and C(22)−N(22)−Cu(5), 160.3(8)°] and significantly more bent in long axial CN bridges [C(21)−N(21)−Cu(4), 143.3(8)° and C(12)−N(12)−Cu(5), 145.9(8)°]. The resulting distances between W and Cu in the W−CN−Cu entities are short for equatorial linkages, 5.20 Å and 5.17 Å, and long for axial linkages, 5.35 Å and 5.32 Å, respectively. To conclude, the chain $\{[Cu^{II}(dien)]_4[W^V(CN)_8]\}^{5+}{}_\infty$ exhibits *two different sets* of W−CN−Cu linkages arranged in an alternate manner: W(1)−C(11)−N(11)−Cu(4) and W(2)−C(22)−N(22)−Cu(5) being shorter and less bent than W(1)−C(12)−N(12)−Cu(5) and W(2)−C(21)−N(21)−Cu(4) (see Figure 1).

The chain $\{[Cu^{II}(dien)]_4[W^V(CN)_8]\}^{5+}{}_\infty$ itself reveals, to the best of our knowledge, the unprecedented 1-dimensional topology (2,8), according to Černák at al.[25] (two neigbours for Cu and 8 neighbors for W), extending the range of 1D topologies observed for cyanido-bridged assemblies: (2,4) in $[Cu^{II}{}_2(dien)_2M^{III}(CN)_6]^+$ (M = Cr, Fe, Co),[9] (2,6) in the very recent case of triple-stranded helical structure $\{[Ni^{II}(tren)]_3[Mo^{IV}(CN)_8]\}^{2+}{}_\infty$ (tren = tris(2-aminoethyl)amine)[26] as well as the overall diversity of topologies observed in octacyanidometalate-based networks.[6e,7a,8a,11,27]

The geometry of $[W(3)(CN)_8]^{3-}$ ions located between the chains are strongly distorted with two of the CN^- ligands, C37N37 and C38N38, represented by four atomic positions with the partial occupancy. The W(3)−C bond lengths in the range 2.127−2.160 Å, C−N bond lengths in the range 1.13−1.16 Å, and W(3)−C−N angles in the range 168.8°−180° (average value 176.2°). The resulting geometry is strongly distorted from ideal SAPR-8, trigonal dodecahedron (TDD-8), and bicapped trigonal prism (BTP-8) polyhedra assuming C37AN37A and C38AN38A (see Supporting Information section).

The local environment of the single chain is presented schematically in Figure 2, and details of the intermolecular contacts and hydrogen bonding network are presented in Supporting Information, Figure S1. The shortest intermolecular contacts are mediated through W(3)···Cu(4) and W(3)···Cu(5) contacts with distances of 5.89 and 6.04 Å, respectively (Supporting Information, Figure S1a). Within this arrangement two oppositely located cyanido ligands of W(3), C(36)−N(36), and C(32)−C(32), point toward the Cu(4) and

dx.doi.org/10.1021/ic101335a |*Inorg. Chem.* 2011, 50, 3213–3222

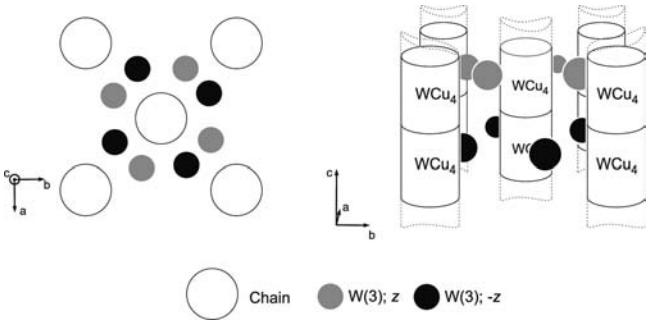

Figure 2. Schematic representation of local environment of the single chain in **1**.

Cu(5) sites of neighboring chains with Cu(4)···N(36) and Cu(5)···N(32) distances of 3.14 Å and 3.38 Å, respectively, and Cu(4)···N(36)−C(36) and Cu(5)···N(32)−C(32) angles of 133.9 and 131.4°, respectively. These Cu···N distances are located beyond the limit of 2.78 Å estimated for semicoordination in $Cu^{II}N_6$ chromophores.[6e,28] Thus, these cyanide ligands can be treated as nonbonded. The other intermolecular contacts are mediated through W···Cu contacts with distances larger than 7.4 Å.

The disordered lattice of water molecules forms an extensive homomeric hydrogen bonding network as well as heteromeric bonding with nitrogen atoms of the $[W(CN)_8]^{3-}$ and the nitrogen atoms of the N−H dien groups (Supporting Information, Figure S1b). The relative donor−acceptor distances for (amine)N−H···O bonds, N···O in the range of 2.90−3.21 Å, (water)O−H···NC−W bonds, O···N in range of 2.71−3.34 Å, and (water)O−H···O(water) bonds: O−H···O of 2.7−3.2 Å)] indicate weak-to-medium hydrogen bonds.[29]

DFT Calculations. Calculations of J values have been realized in the framework of the DFT method, as described in the Computational Methodology section. According to the structure, two different interactions pathways are expected between the W and Cu atoms within the $\{[Cu^{II}(dien)]_4[W^V(CN)_8]\}^{5+}_{\infty}$ chain. In the first approach, we considered the dinuclear species $[(NC)_7-W^V-CN-Cu^{II}(dien)(NC)]^{2-}$. The J_{CuW} values were obtained by considering $E_{HS} - E_{BS} = -J_{CuW}(2S_1S_2 + S_2) = -J_{CuW}$, where S_1 and S_2 are the spins the two metal centers ($S_1 = S_2 = {}^1/_2$) and E_{HS} and E_{BS} are the energies of high spin and magnetic broken-symmetry states, respectively. Following Ruiz et al.,[30] we assumed that the energy of the broken-symmetry state is a good approximation of the low spin state energy. However, the attempts to obtain the J_{CuW} values with this simplified model resulted either in the lack of convergence or in completely unrealistic values.

Therefore, DFT calculations have been performed on the hexanuclear $[(NC)_4-W^V-\{CN-Cu^{II}(L)-NC-\}_4-W^V-(CN)_4]^{2+}$ unit (Figure 3a), involving equatorial and axial cyanido bridges at Cu(II) centers. We have chosen the $\{W_2Cu_4\}$ unit only with Cu−N distances of 1.960 and 2.290 Å and Cu−N−C angles of 166.8 and 143.3°, respectively, without the contribution of other Cu(II) centers. The calculations of three energy states have been performed. The first energy state with all the spins parallel represents the ferromagnetic state. The two other energy states, representing the antiferromagnetic states, have one of the two nonequivalent W atoms bearing one unpaired beta electron and all the other unpaired electrons in their alpha spin states, and allow to calculate the two different J_{CuW} coupling constants. The values obtained for the two coupling constant are $+2.9\ cm^{-1}$ and $+1.5\ cm^{-1}$ assigned to the interaction through the axial and the equatorial cyanide, respectively.

The weak ferromagnetic interaction observed can be rationalized in terms of the concept of magnetic orbitals. Figures 3b−g shows six *unoccupied magnetic spin−orbitals* (UMSOs)[23] computed for the hexanuclear entity. The UMSO definition is discussed in the Computational Methodology section. UMSOs, the unoccupied beta orbitals of the lowest energy, have been drawn preferentially because they are more localized on the metal than their filled alpha counterparts. There are four orbitals mainly localized on the copper atoms and two mainly localized on the tungsten atoms. The molecular orbitals localized mainly on copper result from the mixing of the σ system of the ligands (i.e., the tridentate dien ligand and the N atom of the equatorial bridging cyanide) with the $d_{x^2-y^2}$ orbital of the Cu ions. The molecular orbitals mainly localized on tungsten involve the metal-centered d_{z^2} orbital and some p orbitals of the nitrogen of CN ligands (π system of the cyanide). Interestingly, in the case of the UMSO orbital related to equatorial bridge (Figure 3g) there is a significant delocalization on all the copper and tungsten atoms.

According to Kahn's model,[31] the exchange parameter J can be expressed as the sum of two terms of opposite sign: $J = J_F + J_{AF}$, with $J_F = 2k > 0$ and $J_{AF} = 4\beta s < 0$, where k is the two-electron exchange integral, β is the one-electron resonance integral, and s is the one-electron overlap integral. This expression is valid when two centers, each bearing one localized unpaired electron, are weakly coupled. When localized molecular orbitals have a very small overlap (i.e., $s \approx 0$); the interaction between the two metal atom spin carriers is expected to be ferromagnetic. The unpaired electrons on the W atoms delocalize in cyanide orbitals of local π symmetry. On the other hand, the unpaired electrons originating from the copper atoms delocalize in cyanide orbitals of local σ symmetry. Being delocalized at the level of the cyanide bridging group into orbitals having locally different symmetries the overlap s is indeed expected to be small and the interaction between W and Cu is expected to be ferromagnetic.

The spin density for the ground ferromagnetic state of the hexanuclear entity is presented in the Figure 3h. The positive spin density is observed on both copper and tungsten centers. On the carbon and nitrogen of the nonbridging (in the frame of $\{W_2Cu_4\}$ subunit) cyanides surrounding the W atom, the spin density results from competing mechanisms: delocalization, as expected from molecular orbitals theory, and spin polarization between neighboring atoms ($\uparrow\downarrow\uparrow$). On the N atoms, it is positive and mainly localized in the π system (delocalization and polarization effects are adding), whereas on the C atoms it is negative (delocalization and spin polarization are opposite, delocalization is weak (non bonding cyanide) and negative polarization effects become the most important). On the Cu side, some spin density is delocalized in the σ system of the nitrogen atoms in equatorial position, as expected from classical molecular orbital theory.

Magnetic Properties. Figure 4a shows temperature dependence of the $\chi_M T$ product with molar magnetic susceptibility χ_M calculated per one W_3Cu_4 unit, corresponding to $(H_3O)\{[Cu^{II}(dien)]_4[W^V(CN)_8]\}[W^V(CN)_8]_2 \cdot 6.5H_2O$. On lowering the temperature, $\chi_M T$ increases steadily, which indicates that the dominant interactions in the system are of ferromagnetic character. The inset of Figure 4a depicts thermal variation of the inverse susceptibility $\chi_M{}^{-1}$. It follows a Curie−Weiss law in the

dx.doi.org/10.1021/ic101335a |*Inorg. Chem.* 2011, 50, 3213–3222

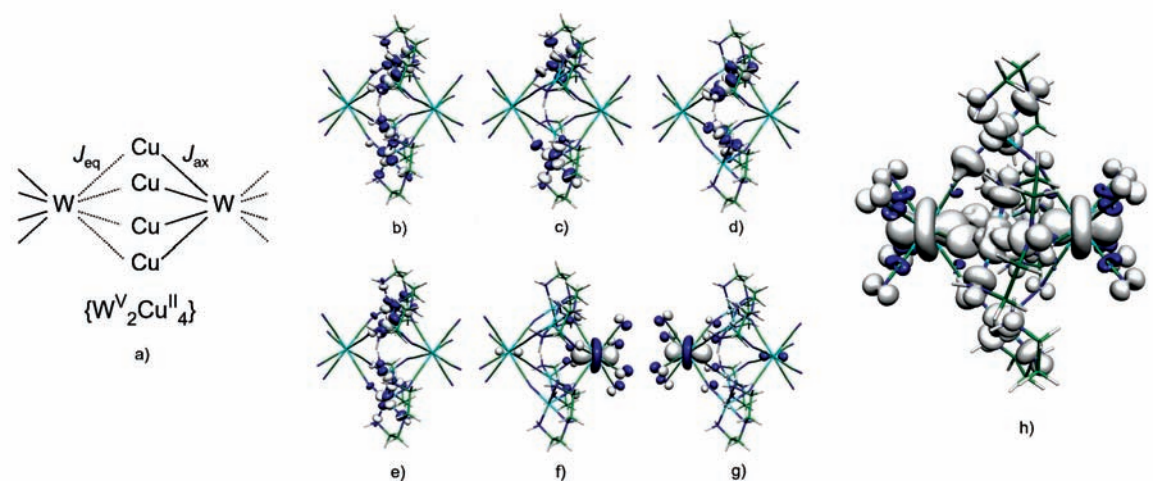

Figure 3. DFT calculations for **1**: (a) schematic representation of the chain fragment $\{W_2Cu_4\}$; (b)−(e) UMSOs for $\{W_2Cu_4\}$ mainly centered on Cu; (f)−(g) UMSOs for $\{W_2Cu_4\}$ mainly centered on W (the two different colors represent the two different signs of the orbitals); (h) spin density for the ground ferromagnetic state of the hexanuclear $\{W_2Cu_4\}$ entity (color code: positive spin density (gray) and negative spin density (blue)).

temperature range 10−300 K with a positive Weiss constant θ = 1.74 (±0.07) K and C = 2.598 (±0.001) cm^3 K mol^{-1}. The value of the C constant is larger than the spin-only value 1.864 cm^3 K mol^{-1} calculated for one W^{V} center with $S_W = {}^1/_2$ and g_W = 1.97 and four Cu^{II} centers with $S_{Cu} = {}^1/_2$ and g_{Cu} = 2.0 of the corresponding WCu_4 chain unit. The discrepancy 0.734 cm^3 K mol^{-1} may be ascribed to the contribution from the two off-chain $[W(CN)_8]^{3-}$ ions carrying spin $S_W = {}^1/_2$ which, assuming the same value for the Landé factor (g_W = 1.97), is estimated to be equal to 0.728 cm^3 K mol^{-1}.

There is no available exact model to treat such a complex system where besides a knotted arrangements of spins within the chains there are isolated $[W(CN)_8]^{3-}$ ions. Nevertheless, even a necessarily approximate approach aimed at rationalizing the magnetic behavior may shed some light on the nature of magnetic interactions in this system. While the intermolecular coupling between the chain segments and off-chain $[W(CN)_8]^{3-}$ entities can be resolved using the mean-field approximation, the calculation of both the temperature dependence of the zero-field susceptibility and the field evolution of the isothermal magnetization pose a challenging problem. To obtain the zero-field susceptibility of the chain segment a semiclassical analytical approach[16] is employed. In this scheme only one out of five ${}^1/_2$ spins of the chain unit WCu_4 is treated as a classical commuting variable, namely, the spin of the W^{V} ion. The calculation of the field dependence of the magnetization is performed by replacing the same spin with the Ising variable and applying the standard transfer matrix technique. The plausibility of the latter approximation rests upon the simple observation that the behavior of a ${}^1/_2$ spin in a magnetic field is equivalent to that of an Ising spin. Both the magnetic characteristics were used independently to get insight into the configuration of magnetic couplings in the system.

The Hamiltonian of the finite chain involving N pentamer units may be written as the sum of partial Hamiltonians

$$H_N = \sum_{i=1}^{N} H_{i,i+1}(\psi_i, \vec{S}_i, \vec{S}_{i+1}, \vec{H}) \qquad (1)$$

where Ψ_i denotes the quantum subsystem of the four Cu^{II} ions within the i-th pentamer, $\vec{S}_i$ denotes the spin of the W^{V} ion of that pentamer, $\vec{H}$ is the external magnetic field, and the partial Hamiltonians read

$$H_{i,i+1} = (\hat{S}_{Cu1i} + \hat{S}_{Cu2i} + \hat{S}_{Cu3i} + \hat{S}_{Cu4i}) \cdot (-J_1 \vec{S}_i - J_2 \vec{S}_{i+1} + \mu_B g_{Cu} \vec{H}) + \mu_B g_w \vec{S}_i \cdot \vec{H} \qquad (2)$$

where isotropic Heisenberg exchange interactions between W^{V} and Cu^{II} centers are assumed and Zeeman terms introduced. Two different exchange coupling constants J_1 and J_2 alternating along the chain as shown in Figure 3b are assumed. The corresponding partition function may be written

$$Z_N(\vec{H}) = \int d\vec{S}_1 \int d\vec{S}_2 \ldots \int d\vec{S}_{N+1} V_{1,2}(\vec{H}) \ldots V_{N,N+1}(\vec{H}) \qquad (3)$$

where $V_{i,i+1}(\vec{S}_i, \vec{S}_{i+1}, \vec{H}) = \mathrm{Tr}\{\exp[-\beta H_{i,i+1}(\Psi_i, \vec{S}_i, \vec{S}_{i+1}, \vec{H})]\}$ and the trace is performed over the degrees of freedom of the quantum subsystem Ψ_i. In eq 3 $\int d\vec{S}_i$ means integrating over all directions available to S_i and $\beta = 1/k_BT$ is the Boltzmann factor.

The zero field magnetic susceptibility is obtained through second order differentiation of $Z_N(\vec{H})$ with respect to H. As argued in ref 16, if only the exchange couplings in the system are isotropic, that calculation can be performed rigorously. Taking in the final step the thermodynamic limit ($N \to \infty$) one obtains the following expression for the zero-field susceptibility of the WCu_4 chain unit

$$\chi_1 = \frac{N_A\mu_B^2}{3k_B}\left[\frac{3}{4}g_W^2 + \frac{3}{2}g_{Cu}^2\rho_0' + \frac{3}{8}\beta^2 g_{Cu}^2(J_1^2\rho_0'' + J_2^2\rho_0'' + 2J_1J_2\rho_1'') + \frac{3}{2}\frac{\rho}{1-\rho}g_w^2\frac{3}{8(1-\rho)}\beta^2 g_{cu}^2(J_1\rho_1' + J_2\rho_0')(J_1\rho_0' + J_2\rho_1') + \frac{3}{4}\frac{1}{1-\rho}\beta g_{Cu}g_W(J_1+J_2)(\rho_0' + \rho_1')\right] \qquad (4)$$

where quantities ρ, ρ_α', and ρ_α'' (α = 0,1) are dimensionless functions of J_1, J_2, and β, and their definitions are provided in the Supporting Information. The susceptibility χ_2 of the two $[W(CN)_8]^{3-}$ ions located at the off-chain positions is given by the paramagnetic Curie law $\chi_2 = N_A\mu_B^2 g_W^2/(2k_BT)$. The total susceptibility arising from the magnetically coupled chain

dx.doi.org/10.1021/ic101335a |*Inorg. Chem.* 2011, 50, 3213–3222

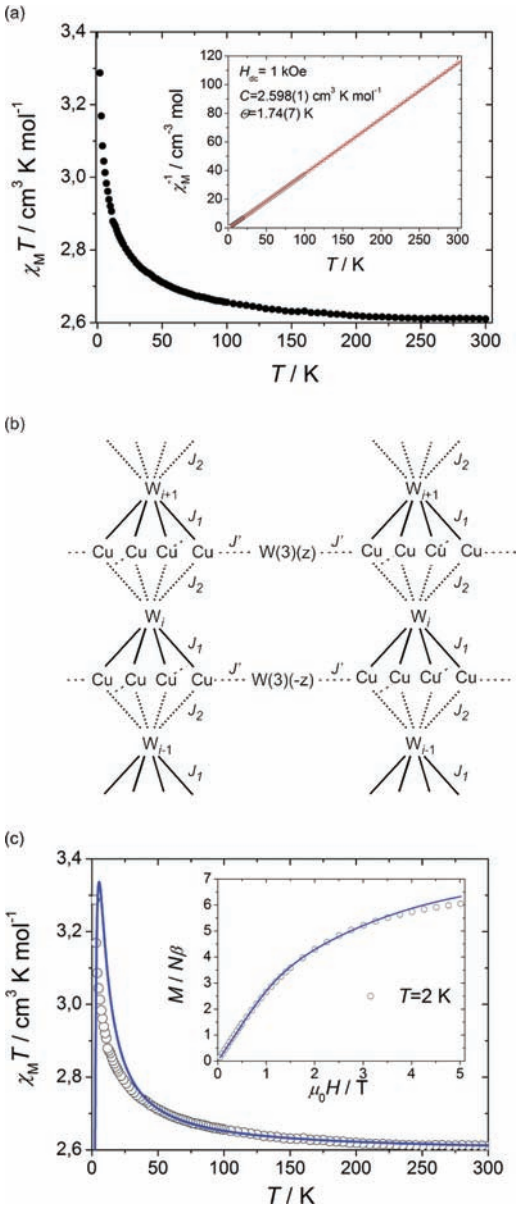

Figure 4. Magnetic properties of **1**: (a) temperature dependence of $\chi_M T$ for **1**, inset: thermal variation of the inverse magnetic susceptibility χ_M^{-1}; (b) schematic representation of the chain model considered in calculations; (c) experimental (○) and computed (solid lines) magnetic data.

segments and $[W(CN)_8]^{3-}$ moieties can be determined approximately within the molecular field theory and is given by the expression (see Supporting Information for its derivation)

$$\chi_M = \frac{\chi_1 + \chi_2 + 2\lambda\chi_1\chi_2}{1 - \lambda^2\chi_1\chi_2} \qquad (5)$$

where $\lambda = zJ'/(N_A\mu_B^2 g_{avg}^2)$ is the molecular field constant, J' the intermolecular coupling constant, and $z = 2$ the number of nearest neighbors which, in agreement with the structural analysis, takes into account that the number of the WCu_4 chain segments lying nearest to the $[W(CN)_8]^{3-}$ ion is 2, whereas the number of the $[W(CN)_8]^{3-}$ ions placed nearest to the WCu_4 chain block is 4. The mean spectroscopic factor is assumed to be equal to $g_{avg} = (g_W g_{Cu})^{1/2}$. The attempts to fit the calculated total susceptibility χ_M in the full temperature range resulted consistently in significant mismatch even at high temperatures. Only after restricting the temperature range to above 50 K were convergent fits obtained. The parameters $J_1 = +7.2(6)$ cm^{-1}, $J_2 = -1.0(5)$ cm^{-1}, and $J' = -0.12(9)$ cm^{-1} yielded the minimal root-mean-square deviation of 0.1%. Figure 4c shows the molar magnetic susceptibility with the best-fit curve. All the fits displayed consistently larger $\chi_M T$ values at low temperature range and significant negative correlation between parameters (J_1, J_2) and parameter J', which means that the decrease of J' would imply the increase of J_1 or/and J_2 to give a reasonable fit. These facts suggest that the coupling J' may be underestimated and (J_1, J_2) may be overestimated, and incorporating the intermolecular coupling J' through the molecular-field approximation may be not sufficiently adequate for this system.

The calculation of field-dependence of the isothermal magnetization for the chain cannot be performed using the scheme presented above, as it becomes analytically intractable for nonzero external magnetic fields. Therefore a different approach has been undertaken in which the spins of the W^V ions are treated as Ising variables. On this assumption a transfer matrix is defined, and its maximal eigenvalue $\Lambda_{max}(H)$ is found (see Supporting Information for details). In the thermodynamic limit ($N \rightarrow \infty$) the magnetization $M_1(H)$ of a WCu_4 chain segment is found with the relation $M_1(H) = N_A\beta^{-1}\partial \ln \Lambda_{max}(H)/\partial H$. The intermolecular coupling between the WCu_4 chain units and the $[W(CN)_8]^{3-}$ ions is again taken into account through the molecular-field approximation. The total molar magnetic moment is written as

$$M(H) = M_1(H + \lambda M_2) + M_2(H + \lambda M_1) \qquad (6)$$

where M_1 is the magnetic moment of the WCu_4 chain unit and M_2 is the magnetic moment of two $[W(CN)_8]^{3-}$ ions, H is the external magnetic field, and λ is the molecular field coefficient ($\lambda = zJ'/(N_A\mu_B^2 g_{avg}^2)$). The magnetic moment of the off-chain $[W(CN)_8]^{3-}$ ions M_2 is assumed to be given by the corresponding Brillouin function[32]

$$M_2(H) = N_A\mu_B g_W \tanh\left(\frac{g_W\mu_B H}{2k_B T}\right) \qquad (7)$$

Molecular field eq 6 was solved iteratively for the total magnetic moment $M(H)$. The best fit was obtained for $J_1 = +4.2(9)$ cm^{-1}, $J_2 = -0.6(1)$ cm^{-1}, and $J' = -0.4(1)$ cm^{-1} yielding the minimal root-mean-square deviation of 3%. Again a negative correlation between parameters (J_1, J_2) and J' was observed. The inset of Figure 4c shows the field dependence of magnetization at $T = 2$ K (circles) with the best-fit curve (solid line). The values of the coupling constants inferred from the magnetization data display a pattern consistent with that found from the χT fit. There is the relatively large ferromagnetic coupling ($J_1 = +4$ to $+7$ cm^{-1}) within the chain alternating with the small antiferromagnetic coupling ($J_2 = -1$ to -0.6 cm^{-1}). Both the data indicate a sizable antiferromagnetic interaction between the chain segments and the off-chain $[W(CN)_8]^{3-}$ ions ($J' = -0.4$ to -0.1 cm^{-1}). The fact that the intermolecular interaction J' was introduced into the models through the approximate molecular-field theory and the observation of negative correlations between parameter J' and parameters J_2 suggest that while the true value of J_2 may be smaller or even change sign, the value of J' may be still underestimated.

dx.doi.org/10.1021/ic101335a |*Inorg. Chem.* 2011, 50, 3213–3222

Table 3. Coordination Polyhedra of $[W(CN)_8]^{3-}$ and Cu(II) Moieties, Coordination Modes, and Geometry of Cyanido-Bridges and Intramolecular J_{CuW} Coupling Constants for 1 and the Selected Reference Compounds[7a,8c−8e]

compound	$W(CN)_8]^{3-}$ polyhedron[a]	Cu(II) polyhedron[b]	W−C/Å	Cu−N/Å	Cu−N−C/deg	W···Cu/Å	$J_{CuW,Mo}$[c]/cm^{-1}	$J_{CuW,Mo}$[d]/cm^{-1}	ref.
1	SAPR-8	SPY-5(*eq*)	2.156	1.960	166.8	5.20	−1.0 to −0.6	$+1.5^{d1}$	this work
	SAPR-8	SPY-5(*ax*)	2.151	2.290	143.3	5.35	+4 to +7	$+2.9^{d1}$	
DyCuLMo	SAPR-8	SPY-5(*ax*)	2.158	2.319	138.4	5.22	−8.0	$+1.5^{d2}$	7a
	SAPR-8	SPY-5(*ax*)	2.153	2.390	143.5	5.42	+11.8	$+5.2^{d2}$	
WCutren	TPRS-8(*c*)	TBP-5(*ax*)	2.210	1.958	161.8	5.20	+5.8(1)		8c
WCu-2,2′bpy	SAPR-8	TBP-5(*eq*)	2.166	2.017	173.1	5.32	+35(7)	$+31^{d1}$	
	SAPR-8	TBP-5(*eq*)	2.166	2.003	176.1	5.31			8d
	SAPR-8	TBP-5(*eq*)	2.168	1.996	173.4	5.28			
WCuphen	TPRS-8(*b*)	elongated octahedron(*eq*)	2.161	1.976	169.5	5.25	+39(4)	$+13^{d1}$	8d
W_7Cu_{13}	SAPR-8	SPY-5(*eq*)	2.187	1.963	163.2	5.28	+39.6		8e
	SAPR-8	elongated octahedron(*ax*)	2.174	2.248	171.5	5.59	+7.4		

[a] In W,Mo(V) moieties $(d_{z^2})^1$ configuration is assumed for SAPR-8 geometry and $(d_{z^2} - d_{x^2-y^2})^1$ configuration is assumed for TPRS-8 polyhedra geometry, (*b*) and (*m*) denote different vertices of TPRS-8 polyhedron. [b] In Cu(II) moieties $(d_{x^2-y^2})^1$ configuration is assumed for SPY-5 or elongated octahedron geometry and $(d_{z^2})^1$ is assumed for TBP-5 geometry, (ax) and (eq) denotes axial and equatorial positions, respectively. [c] Estimated from magnetic data $\chi T(T)$ and/or $M(H)$. [d] Estimated by broken symmetry DFT calculations with $J = E_{BS} - E_{HS}$ (*d1*) or $J = 2(E_{BS} - E_{HS})$(*d2*).

Discussion. The coupling constants $J_1 = +4$ to $+7$ cm^{-1} obtained from magnetic calculations is in a good agreement with coupling constants $J_{ax} = +2.9$ cm^{-1} calculated by the DFT method. Concerning the interaction through the equatorial bridge, the DFT method ($J_{eq} = +1.5$ cm^{-1}) and magnetic fitting ($J_2 = -1.0$ to -0.6 cm^{-1}) do not fully coincide. The coupling between the chains and the nonbridging $[W(CN)_8]^{3-}$ moieties considered only in magnetic calculations was found to be antiferromagnetic of order of -0.4 to -0.1 cm^{-1}.

Both methods reflect the domination of weak ferromagnetic interactions within $\{[Cu^{II}(dien)]_4[W^V(CN)_8]\}^{5+}{}_\infty$ chain. This may be interpreted in terms of Kahn's model. The π-systems arising from $d_{z^2}(W)$ and $\pi^*(CN^-)$ orbitals is orthogonal to the σ-system derived from $d_{x^2-y^2}(Cu)$ and $\sigma(CN^-)$ orbitals, which is responsible for the ferromagnetic character of interactions. Decreasing the Cu−N distance *only* would imply the increase of the interactions. However, significant deviations form linearity of the Cu−N−C angle may result in the appearance of nonzero overlap between these orbital systems. This produces antiferromagnetic contribution to the overall J value, as it was shown previously[33] in two independent studies on discrete cyanido-bridged $Ni^{II}[Cr^{III}(CN)_6]$ systems with nominally orthogonal sets of interacting orbitals derived from $t_{2g}{}^6e_g{}^2(Ni^{II})$ and $t_{2g}{}^3$-(Cr^{III}) configurations. The effective J value of about $+25$ cm^{-1} estimated for the strictly orthogonal orientation (Ni−N−C and Cr−C−N angles of 180°) experienced a significant decrease with the decreasing Ni−N−C angle to reach finally the antiferromagnetic region below a Ni−N−C angle of about 140°. The same trend was rationalized for cyanido-bridged dinuclear $Ni^{II}W^V$ or $Ni^{II}Mo^V$ units using broken symmetry DFT calculations.[34] In such cases, the decrease in M−N distance would imply a closer approach of overlapping orbital systems and enhance the angular effect leading to the increase of J_{AF} contribution to overall interaction.[33c] In the case of **1**, two sets of Cu−NC−W linkages are observed: the *equatorial* ones, with small bending (Cu−N−C angles of 166.7° and 160.2°) and short Cu−N distances (1.960 Å and 1.969 Å), and the *axial* linkages with large bending (Cu−N−C angles of 143.3° and 145.9°) and long Cu−N distances (2.290 Å and 2.233 Å). In both types of W−CN−Cu linkages some antiferromagnetic contribution is likely. For the equatorial linkages a small angular effect may be enhanced by short Cu−N distance. For the axial linkages a strong angular effect may be only very weakly (or not at all) augmented by long Cu−N distance. Both effects are qualitatively consistent with the observed J_{CuW} values. Relatively small positive J value for the equatorial linkage can also be understood in terms of a significant delocalization of one of the UMSO (Figure 3g) on all the copper and tungsten atoms in $\{W_2Cu_4\}$ fragment.

In this context, the combined results obtained from DFT calculations and magnetic fitting models give the consistent description of the magnetic behavior of **1**. Both approaches reveal some intrinsic limitations, which may be generally related to the nontrivial topology of the chain and complexity of 3D architecture of **1**. DFT calculations were performed for the $[(NC)_4\text{-}W^V\text{-}\{CN\text{-}Cu^{II}(L)\text{-}NC\text{-}\}_4\text{-}W^V\text{-}(CN)_4]^{2+}$ hexanuclear unit in the $\{WCu_4\}_n$ chain, and neither extended intramolecular interactions nor intermolecular interactions could be taken into account. The magnetic model, while allowing for a reliable estimation of magnetic coupling within the full chain segment $\{WCu_4\}_N$ ($N \rightarrow \infty$) by two independent procedures for $\chi T(T)$ and $M(H)$, gives only the approximate description of interaction between $\{WCu_4\}_n$ chains and ionic $[W(3)(CN)_8]^{3-}$. This is particularly illustrated by colinearity of experimental and calculated $\chi T(T)$ curves above 50 K and their divergence below this point. It should be pointed out that *if* the full exact model for J_1, J_2, and J' parameters was considered the value J_2 could possibly be even a small positive value, and thus in perfect agreement with the value of J_{eq} found by DFT calculation.

The Table 3 collects the key parameters controlling magnetic Cu^{II}−NC−M^V interactions in selected Cu^{II}-$[M(CN)_8]^{3-}$ assemblies. It consists of the type of coordination polyhedra, coordination sites for CN-bridging, and metric parameters of bridging linkages. These parameters determine the orientation and separation between interacting magnetic orbitals and the degree of spin density delocalization from the original magnetic orbitals in 3d metal-$[M(CN)_8]$ assemblies.[8d,24,34,35] The Cu^{II}-M^V interactions are generally ferromagnetic; however, this set of data does not allow for unequivocal evaluation of the nature and strength of interaction judging from the metric parameters only.

dx.doi.org/10.1021/ic101335a |*Inorg. Chem.* 2011, 50, 3213–3222

Nevertheless, the application of DFT method gives the values of Cu^{II}-M^{V} magnetic coupling constants consistent with those obtained from magnetic fitting.

CONCLUSIONS

Unprecedented (2,8) topology of the knotted chain $\{[Cu^{II}(dien)]_4[W^{V}(CN)_8]\}^{5+}_{\infty}$ gave an opportunity to study the magnetic exchange interactions in **1**. Within the chain, two types of interactions are due to the presence of two different types of W−CN−Cu linkages. Broken symmetry DFT calculations for hexanuclear $\{W_2Cu_4\}$ fragment gave two values of coupling constants: $J_{ax} = +2.9\ cm^{-1}$ assigned to long and strongly bent axial cyanido-bridged linkage, whereas $J_{eq} = +1.5\ cm^{-1}$ is assigned to short and less bent equatorial linkage. The independent calculations of magnetic susceptibility and magnetization resulted in different coupling constants for axial and equatorial W−CN−Cu linkages, confirmed the domination of weak ferromagnetic interactions within the chain, and suggest very weak antiferromagnetic interaction between chains and nonbridging $[W(3)(CN)_8]^{3-}$ anions. The combination of DFT and magnetic fitting approaches give the consistent and reliable description of magnetic interactions $\{WCu_4\}_n$ chain as well as in the whole compound.

ASSOCIATED CONTENT

Supporting Information. CIF file, detailed bond lengths and angles, SHAPE parameters for $[W(CN)_8]^{3-}$ moieties, image of noncovalent intermolecular interactions, detailed definitions of procedures used for calculations of $\chi T(T)$ and $M(H)$ for **1**. This material is available free of charge via the Internet at http://pubs.acs.org.

AUTHOR INFORMATION

Corresponding Author
*E-mail: barbara.sieklucka@uj.edu.pl.

ACKNOWLEDGMENT

The paper is dedicated to the late Yves Dromzée (Université Pierre et Marie Curie, Paris, France) who was implied in preliminary crystallographic work on **1**. The authors acknowledge Katarzyna Stadnicka (Faculty of Chemistry, Jagiellonian University, Kraków, Poland) for discussion of the crystal structure of **1** and Fabrizia Fabrizzi de Biani (University of Siena, Italy) for discussion of the theoretical models. The authors acknowledge Miguel Llunell and Santiago Alvarez for making available the SHAPE programme v.2.0 and helpful discussions. They acknowledge computational facilities provided by the M3PEC-Mésocentre of the University Bordeaux 1, financed by the "Conseil Régional d'Aquitaine" and the French Ministry of Research and Technology. Authors also thank the CINES-Centre Informatique National de l'Enseignement Supérieur for computational facilities. This work was partially supported by the Sixth Framework Programme, NoE Project MAGMANet (Contract No. NMP3-CT-2005-515767), by the Polish Ministry of Science and Higher Education within Research Projects 1535/B/H03/2009/36 and 0087-B-H03-2008-34 and by the International PhD-studies Programme at the Faculty of Chemistry, Jagiellonian University, within the Foundation for Polish Science MPD Programme cofinanced by the EU European Regional Development Fund. The research was partially carried out with the equipment purchased thanks to the financial support of the European Regional Development Fund in the framework of the Polish Innovation Economy Operational Program (contract no. POIG.02.01.00-12-023/08).

REFERENCES

(1) (a) Shatruk, M.; Avendano, C.; Dunbar, K. R. *Progress in Inorganic Chemistry*; Karlin, K. D., Ed.; John Wiley & Sons: New York, 2009; Vol. 56, pp 155−334. (b) Sieklucka, B.; Podgajny, R.; Przychodzeń, P.; Korzeniak, T. *Coord. Chem. Rev.* **2005**, *249*, 2203–2221. (c) Przychodzeń, P.; Korzeniak, T.; Podgajny, R.; Sieklucka, B. *Coord. Chem. Rev.* **2006**, *250*, 2234–2260. (d) Sieklucka, B.; Podgajny, R.; Korzeniak, T.; Nowicka, B.; Pinkowicz, D.; Kozieł, M. *Eur. J. Inorg. Chem.* **2011**, 305–326.

(2) (a) Ohkoshi, S.; Arimoto, Y.; Hozumi, T.; Seino, H.; Mizobe, Y.; Hashimoto, K. *Chem. Commun.* **2003**, 2772–2773. (b) Li, D.; Zheng, L.; Wang, X.; Huang, J.; Gao, S.; Tang, W. *Chem. Mater.* **2003**, *15*, 2094–2098. (c) Podgajny, R.; Korzeniak, T.; Bałanda, M.; Wasiutyński, T.; Errington, W.; Kemp, T. J.; Alcock, N. W.; Sieklucka, B. *Chem.Commun.* **2002**, 1138–1139. (d) Korzeniak, T.; Podgajny, R.; Alcock, N. W.; Lewiński, K.; Bałanda, M.; Wasiutyński, T.; Sieklucka, B. *Polyhedron* **2003**, *22*, 2183–2191. (e) Kaneko, S.; Tsunobuchi, Y.; Sakurai, S.; Ohkoshi, S. *Chem. Phys. Lett.* **2007**, *446*, 292–296. (f) Podgajny, R.; Chmel, N. P.; Bałanda, M.; Tracz, P.; Gaweł, B.; Zajac, D.; Sikora, M.; Kapusta, C.; Łasocha, W.; Wasiutyński, T.; Sieklucka, B. *J. Mater. Chem.* **2007**, *17*, 3308–3314. (g) Ohkoshi, S.; Tsunobuchi, Y.; Takahashi, H.; Hozumi, T.; Shiro, M.; Hashimoto, K. *J. Am. Chem. Soc.* **2007**, *129*, 3084–3085. (h) Higashikawa, H.; Okuda, K.; Kishine, J.; Masuhara, N.; Inoue, K. *Chem. Lett.* **2007**, *36*, 1022–1023.

(3) (a) Sieklucka, B.; Korzeniak, T.; Podgajny, R.; Bałanda, M.; Nakazawa, Y.; Myiazaki, Y.; Sorai, M.; Wasiutyński, T. *J. Magn. Magn. Mater.* **2004**, *272−276*, 1058–1059. (b) Bałanda, M.; Korzeniak, T.; Pełka, R.; Podgajny, R.; Rams, M.; Sieklucka, B.; Wasiutyński, T. *Solid State Sci.* **2005**, *7*, 1113–1124. (c) Pratt, F. L.; Zieliński, P. M.; Bałanda, M.; Podgajny, R.; Wasiutyński, T.; Sieklucka, B. *J. Phys.: Condensed Matter* **2007**, *19*, 456208. (d) Bałanda, M.; Pełka, R.; Wasiutyński, T.; Rams, M.; Nakazawa, Y.; Miyazaki, Y.; Sorai, M.; Podgajny, R.; Korzeniak, T.; Sieklucka, B. *Phys. Rev. B* **2008**, *78*, 174409.

(4) (a) Hozumi, T.; Hashimoto, K.; Ohkoshi, S. *J. Am. Chem. Soc.* **2005**, *127*, 3864–3869. (b) Ohkoshi, S.; Tokoro, H.; Hozumi, T.; Zhang, Y.; Hashimoto, K.; Mathonière, C.; Bord, I.; Rombaut, G.; Verelst, M.; Cartier dit Moulin, C.; Villain, F. *J. Am. Chem. Soc.* **2006**, *128*, 270–277.

(5) (a) Sato, O.; Tao, J.; Zhang, Y. Z. *Angew. Chem., Int. Ed.* **2007**, *46*, 2152–2187. (b) Kaneko, W.; Ohba, M.; Kitagawa, S. *J. Am. Chem. Soc.* **2007**, *129*, 13706–13712. (c) Ohba, M.; Kaneko, W.; Kitagawa, S.; Maeda, T.; Mito, M. *J. Am. Chem. Soc.* **2008**, *130*, 4475–4484. (d) Milon, J.; Daniel, M. Ch.; Kaiba, A.; Guionneau, P.; Brandes, S.; Sutter, J.-P. *J. Am. Chem. Soc.* **2007**, *129*, 13872–13878. (e) Sieklucka, B.; Podgajny, R.; Pinkowicz, D.; Nowicka, B.; Korzeniak, T.; Bałanda, M.; Wasiutyński, T.; Pełka, R.; Makarewicz, M.; Czapla, M.; Rams, M.; Gaweł, B.; Łasocha, W. *CrystEngComm* **2009**, *11*, 2032–2039.

(6) (a) Herrerra, J. M.; Marvaud, V.; Verdaguer, M.; Marrot, J.; Kalisz, M.; Mathoniere, C. *Angew. Chem., Int. Ed.* **2004**, *43*, 5468–5471. (b) Rajamani, R.; Ramasesha, S.; Mathoniere, C.; Marvaud, V. *Phys. Rev. B* **2006**, *73*, 045131. (c) Rajamani, R.; Ramasesha, S.; Mathoniere, C.; Marvaud, V. *Phys. Chem. Chem. Phys.* **2008**, *10*, 5469–5474. (d) Maxim, C.; Mathoniere, C.; Andruh, M. *Dalton Trans.* **2009**, 7805–7810. (e) Long, J.; Chamoreau, L.-M.; Mathoniere, C.; Marvaud, V. *Inorg. Chem.* **2009**, *48*, 22–24. (f) Arrio, M.-A.; Long, J.; Cartier dit Moulin, C.; Bachschmidt, A.; Marvaud, V.; Rogalev, A.; Mathoniere, C.; Wilhelm, F.; Sainctavit, P. *J. Phys. Chem. C* **2010**, *114*, 593–600.

(7) (a) Visinescu, D.; Madalan, A. M.; Andruh, M.; Duhayon, C.; Sutter, J.-P.; Ungur, L.; Van den Heuvel, W.; Chibotaru, L. F. *Chem.—Eur. J.* **2009**, *15*, 11808–11814. (b) Long, J.; Chamoreau, L.-M.; Marvaud, V. *Dalton Trans.* **2010**, *39*, 2188–2190.

(8) (a) You, Y. S.; Kim, D.; Do, Y.; Oh, S. J.; Hong, Ch. S. *Inorg. Chem.* **2004**, *43*, 6899–6901. (b) Korzeniak, T.; Stadnicka, K.; Rams, M.; Sieklucka, B. *Inorg. Chem.* **2004**, *43*, 4811–4813. (c) Korzeniak, T.; Stadnicka, K.; Pełka, R.; Bałanda, M.; Tomala, K.; Kowalski, K.; Sieklucka, B. *Chem. Commun.* **2005**, 2939–2941. (d) Korzeniak, T.; Desplanches, C.; Podgajny, R.; Gimènez-Saiz, C.; Stadnicka, K.; Rams, M.; Sieklucka, B. *Inorg. Chem.* **2009**, *48*, 2865–2872. (e) Wang, J.; Zhang, Z.-C.; Wang, H.-S.; Kang, L.-C.; Zhou, H.-B.; Song, Y.; You, X.-Z. *Inorg. Chem.* **2010**, *49*, 3101–3103.

(9) (a) Kou, H. Z.; Liao, D. Z.; Cheng, P.; Jiang, Z. H.; Yan, S. P.; Wang, G. L.; Yao, X. K.; Wang, H. G. *J. Chem. Soc., Dalton Trans.* **1997**, 1503–1506. (b) Fu, D. G.; Chen, J.; Tan, X. S.; Jiang, L. J.; Zhang, S. W.; Zheng, P. J.; Tang, W. X. *Inorg. Chem.* **1997**, *36*, 220–225. (c) Ferbinteanu, M.; Tanase, St.; Andruh, M.; Journaux, Y.; Cimpoesu, F.; Strenger, I.; Riviere, E. *Polyhedron* **1999**, *18*, 3019–3025.

(10) Bok, L. D. C.; Leipoldt, J. G.; Basson, S. S. *Z. Anorg. Allg. Chem.* **1975**, *415*, 81–83.

(11) Podgajny, R.; Korzeniak, T.; Stadnicka, K.; Dromzee, Y.; Alcock, N. W.; Errington, W.; Kruczała, K.; Bałanda, M.; Kemp, T. J.; Verdaguer, M.; Sieklucka, B. *Dalton Trans.* **2003**, 3458–3468.

(12) McArdle, P. *J. Appl. Crystallogr.* **1996**, *29*, 306.

(13) Altomare, M.; Burla, M. C.; Camalli, M.; Cascarano, G. L.; Giacovazzo, C.; Guagliardi, A.; Moliterni, A. G. G.; Polidori, G.; Spagna, R. *J. Appl. Crystallogr.* **1999**, *32*, 115.

(14) Sheldrick, G. M. *Acta Crystallogr., Sect. A* **2008**, *A64*, 112.

(15) Llunell, M.; Casanova, D.; Cirera, J.; Alemany, M. P.; Alvarez, S. *SHAPE*, v. 2.0; Program for the Stereochemical Analysis of Molecular Fragments by Means of Continuous Shape Measures and Associated Tools; Departament de Química Física, Departament de Química Inorgànica, and Institut de Química Teòrica i Computacional, Universitat de Barcelona: Barcelona, Spain, 2010.

(16) Curély, J.; Georges, R. *Phys. Rev. B* **1992**, *46*, 3520.

(17) (a) Ruiz, E.; Gopalan, G.; Alvarez, S.; Gillon, B.; Stride, J.; Clerac, R.; Larionova, J.; Decurtins, S. *Angew. Chem., Int. Ed.* **2005**, *44*, 2711–2715. (b) Desplanches, C.; Ruiz, E.; Alvarez, S. *Eur. J. Inorg. Chem.* **2003**, 1756–1760. (c) Low, D.; Rajaraman, G.; Helliwell, M.; Walsmann, O.; Gudel, H.; Adams, M.; Ruiz, E.; Alvarez, S.; McInnes, E. *Chem.—Eur. J.* **2006**, *12*, 1385–1396. (d) Ruiz, E.; Nunzi, F.; Alvarez, S. *Nano Lett.* **2006**, *6*, 380–384.

(18) (a) Becke, A. D. J. *J. Chem. Phys.* **1993**, *98*, 5648–5652. (b) Lee, C.; Yang, W.; Parr, R. G. *Phys. Rev. B* **1998**, *37*, 785–789.

(19) Dunning, T. H. J.; Hay, P. J. In *Modern Theoretical Chemistry*; Schaefer, H. F., III, Ed.; Plenum: New York, 1976; Vol. 3.

(20) Hay, P. J.; Wadt, R. *J. Chem. Phys.* **1985**, *82*, 299–310.

(21) Ruiz, E.; Rodriguez-Fortea, A.; Cano, J.; Alvarez, S.; Alemany, P. *J. Comput. Chem.* **2003**, *24*, 982–989.

(22) Frisch, M. J. T. et al. *Gaussian03*; Gaussian, Inc.: Pittsburgh, PA, 2004.

(23) Desplanches, C.; Ruiz, E.; Rodriguez-Fortea, A.; Alvarez, S. *J. Am. Chem. Soc.* **2002**, *124*, 5197–5205.

(24) Visinescu, D.; Desplanches, C.; Imaz, I.; Bahers, V.; Pradhan, R.; Villamena, F. A.; Guionneau, P.; Sutter, J.-P. *J. Am. Chem. Soc.* **2006**, *128*, 10202–10212.

(25) Černák, J.; Orendáč, M.; Potočňák, I.; Chomič, J.; Orendačová, A.; Skorupa, J.; Feher, A. *Coord. Chem. Rev.* **2002**, *224*, 51–66.

(26) Zhang, W.; Wang, Z.-Q.; Sato, O.; Xiong, R.-G. *Cryst. Growth Des.* **2009**, *9*, 2050–2053.

(27) (a) Withers, J. R.; Ruschman, Ch.; Parkin, S.; Holmes, S. M. *Polyhedron* **2005**, *24*, 1845–1854. (b) Matoga, D.; Mikuriya, M.; Handa, M.; Szklarzewicz, J. *Chem. Lett.* **2005**, *34*, 1550–1551. (c) Zhao, H.; Shatruk, M.; Prosvirin, A. V.; Dunbar, K. R. *Chem.—Eur. J.* **2007**, 6573–6589. (d) Venkatakrishnan, T. S.; Sahoo, S.; Brefuel, N.; Duhayon, C.; Paulsen, C.; Barra, A.-L.; Ramasesha, S.; Sutter, J.-P. *J. Am. Chem. Soc.* **2010**, *132*, 6047–6056.

(28) Valach, F. *Polyhedron* **1999**, *18*, 699–706.

(29) Steiner, T. *Angew. Chem., Int. Ed.* **2002**, *41*, 48–76.

(30) (a) Ruiz, E.; Cano, J.; Alvarez, S.; Alemany, P. *J. Comput. Chem.* **1999**, *20*, 1391–1400. (b) Ruiz, E.; Alvarez, S.; Cano, J.; Polo, V. *J. Chem. Phys.* **2005**, *123*, 164110.

(31) Kahn, O. *Molecular Magnetism*; VCH Publishers: New York, 1993; Chapter 8.4.2.

(32) Kahn, O. *Molecular Magnetism*; VCH Publishers: New York, 1993; Chapter 2.1.

(33) (a) Toma, L.; Toma, L. M.; Lescouëzec, R.; Armentano, D.; De Munno, G.; Andruh, M.; Cano, J.; Lloret, F.; Julve, M. *Dalton Trans.* **2005**, 1357–1364. (b) Zhang, Y. Z.; Gao, S.; Wang, Z. M.; Su, G.; Sun, H. L.; Pan, F. *Inorg. Chem.* **2005**, *44*, 4534–4545. (c) Tuyèras, F.; Scuiller, A.; Duhayon, C.; de Biani, F. F.; Verdaguer, M.; Mallah, T.; Wernsdorfer, W.; Marvaud, V. *Inorg. Chim. Acta* **2008**, *361*, 3505–3518.

(34) (a) Zhang, Y. Q.; Luo, C. L. *Dalton Trans.* **2008**, 4575–4584. (b) Zhang, Y. Q.; Luo, C. L. *Eur. J. Inorg. Chem.* **2008**, 2199–2206.

(35) (a) Ruiz, E.; Rajaraman, G.; Alvarez, S.; Gillon, B.; Stride, J.; Clerac, R.; Larionova, J.; Decurtins, S. *Angew. Chem., Int. Ed.* **2005**, *44*, 2711–2715. (b) Podgajny, R.; Pinkowicz, D.; Korzeniak, T.; Nitek, W.; Rams, M.; Sieklucka, B. *Inorg. Chem.* **2007**, *46*, 10416–10425. (c) Pinkowicz, D.; Podgajny, R.; Nitek, W.; Makarewicz, M.; Czapla, M.; Mihalik, M.; Bałanda, M.; Sieklucka, B. *Inorg. Chim. Acta* **2008**, *361*, 3957–3962. (d) Venkatakrishnan, T. S.; Desplanches, C.; Rajamani, R.; Guionneau, P.; Ducasse, L.; Ramasesha, S.; Sutter, J.-P. *Inorg. Chem.* **2008**, *47*, 4854–4860.